

# Seed population in large Solar Energetic Particle events and the twin-CME scenario

Liu-Guan Ding<sup>1</sup>, Gang Li<sup>2,\*</sup>, Gui-Ming Le<sup>3</sup>, Bin Gu<sup>1</sup>, Xin-Xin Cao<sup>1</sup>

## ABSTRACT

It has been recently suggested that large solar energetic particle (SEP) events are often caused by twin CMEs. In the twin-CME scenario, the preceding CME is to provide both an enhanced turbulence level and enhanced seed population at the main CME-driven shock. In this work, we study the effect of the preceding CMEs on the seed population. We examine event-integrated abundance of iron to oxygen ratio (Fe/O) at energies above 25 MeV/nuc for large SEP events in solar cycle 23. We find that the Fe/O ratio (normalized to the reference coronal value of 0.134)  $\leq 2.0$  for almost all single-CME events and these events tend to have smaller peak intensities. In comparison, the Fe/O ratio of twin-CME events scatters in a larger range, reaching as high as 8, suggesting the presence of flare material from perhaps preceding flares. For extremely large SEP events with peak intensity above 1000 pfu, the Fe/O drop below 2, indicating that in these extreme events the seed particles are dominated by coronal material than flare material. The Fe/O ratios of Ground level enhancement (GLE) events, all being twin-CME events, scatter in a broad range. For a given Fe/O ratio, GLE events tend to have larger peak intensities than non-GLE events. Using velocity dispersion analysis (VDA), we find that GLE events have lower solar particle release (SPR) heights than non-GLE events, agreeing with earlier results by Reames (2009b).

*Subject headings:* Solar Energetic Particle, seed population, Coronal Mass Ejection, solar flare, twin CME

---

<sup>1</sup>School of Physics and Optoelectronic Engineering, Institute of Space Weather, Nanjing University of Information Science & Technology, Nanjing, Jiangsu, 210044, China

<sup>2</sup>Department of Space Science and CSPAR, University of Alabama in Huntsville, AL, 35899, USA \*send correspondence to: gangli.uah@gmail.com

<sup>3</sup>National Center for Space Weather, China Meteorological Administration, Beijing, 100081, China

## 1. Introduction

Solar energetic particles (SEPs) is a major concern of space physics and space weather. The energy of SEPs in large SEP events, and in particular ground level enhancement (GLE) events, can reach up to  $\sim$ GeV/nuc. These particles are believed to be produced at and near the Sun mainly via two processes: solar flares and coronal mass ejections (CMEs). Historically, SEP events are classified as “impulsive” and “gradual” events depending on the duration of the associated soft X-ray observations. It was later used to refer to events where the particle acceleration process occurs at flares and CME-driven shocks, respectively (Cane et al. 1986; Reames 1995, 1999).

The most intense SEP events are almost always associated with fast and wide CMEs (Kahler et al. 1984; Reames 1995; Kahler 1996; Gopalswamy et al. 2002; Cliver et al. 2004; Tylka et al. 2005; Kahler & Vourlidas 2013). However, not all fast and wide CMEs lead to large SEP events (Kahler 1996; Ding et al. 2013). An earlier study by Kahler (1996) showed that both the maximum energy and the intensity of energetic particles in SEP events tend to correlate with shock speed. Later, Kahler et al. (2000) suggested that the ambient energetic particle intensity prior to the event may be an important factor in causing a large SEP event. These seed population may be from previous flare remanet materials or ambient corona materials (Mason et al. 1999, 2000; Gopalswamy et al. 2004; Li et al. 2012; Ding et al. 2013).

Gopalswamy et al. (2004) noted first that there is a strong correlation between high particle intensity events and the existence of preceding CMEs within 24 hrs ahead of the primary CMEs. Gopalswamy et al. (2004) also noted that the SEP intensity showed poor correlation with the flare class. Li & Zank (2005a) proposed that two consecutive CMEs may provide a favorable environment for particle acceleration. This was refined in Li et al. (2012) as the twin-CME scenario. In Li et al. (2012), the authors studied all 16 GLE events in solar cycle 23 and found that there were always preceding CMEs within a short period (9 hrs) of the main fast CMEs. Li et al. (2012) proposed that when two CMEs erupt in sequence from the same or nearby active regions (ARs) within a short period of time, the preceding CME-driven shock can enhance the turbulence level at the main CME-driven shocks through Alfvén wave excitation, and increase the seed population at the second shock through pre-acceleration at the preceding shock and/or flare. Both enhanced turbulence level and enhanced seed population will favor a more efficient particle acceleration process at the second shock, leading to large SEP or GLE events.

Extending the work of Li et al. (2012), Ding et al. (2013) examined the twin-CME scenario against all large SEP events and fast CME ( $> 900$ km/s) having western hemisphere source regions in solar cycle 23. They found that 61% twin CMEs lead to large SEP events

as compared to only 29% single fast CMEs leading to large SEP events. Furthermore, of all western large SEP events, 73% are twin CMEs. These findings support the proposal that twin-CMEs are responsible for large SEP events. For the twin-CME scenario to work, the preceding CME can not be too far from the main CME. For if so, both the enhanced turbulence level and the enhanced seed population may decay. In the work of Ding et al. (2014), the authors refined the time interval threshold on the identification of the twin-CME scenario to be 13 hrs.

The relative abundances of different elements in SEP events provide important clues about the seed populations. For example, at 1 to several MeV/nuc, impulsive events often has a large  ${}^3\text{He}/{}^4\text{He}$  ratio than the solar wind since  ${}^3\text{He}$  is considered a tracer element of solar flares (Reames et al. 1990). Flares also tend to have higher Fe/O ratio than corona. A widely used coronal Fe/O ratio is 0.134, a value derived by Reames (1998), who added together all particle counts in 49 large solar particle events in the range 5-12MeV/nuc to obtain this reference value. For events of which the Fe/O ratio is considerably higher than the corona value, and/or the abundance ratio of  ${}^3\text{He}/{}^4\text{He}$  is higher than the solar wind value, one may expect that the seed particles to be dominated by plasma that has been heated by the accompanying solar flares or preheated by preceding flares. On the other hand, if the Fe/O ratio is close to the coronal value, one may expect that the seed particle to be of normal coronal and/or solar wind material.

People have used different thresholds of Fe/O ratio to infer the presence or absence of impulsive flare material. Reames et al. (1990) have used 1.7 (normalized to the coronal value of 0.134) as the threshold for the energy range of 1.9-2.8 MeV/nuc. Later, Reames & Ng (2004) suggested that the normalized values of Fe/O ratio in large “impulsive” events to be 3.3. More recently, Cane et al. (2006) used a normalized Fe/O ratio of 2.0 as the indication of flare-like material in the energy range of 25-80 MeV/nuc. In this work, we follow Cane et al. (2006) and use a Fe/O ratio of 2.0 as our threshold for the presence of flare material. We use the same energy range of 25-80 MeV/nuc as Cane et al. (2006). Note that, as shown in Tylka et al. (2005) (their figure 1), the Fe/O for two otherwise similar events can differ substantially above about 10 MeV/nuc. Tylka & Lee (2006) suggested that this difference might be due to difference in shock obliquity. As argued by Tylka & Lee (2006), the injection energy of a quasi-perpendicular shock can be much larger than a quasi-parallel shock and consequently, the seed population at a quasi-perpendicular shock can be more flare-like than a quasi-parallel shock. However, simulations by Giacalone & Ellison (2000); Giacalone (2005a,b) suggested that the injection energy may not depend strongly on the shock obliquity. In any events, we point out that the Fe/O ratio above 10 MeV/nuc can vary largely from event to event and this is the main source of uncertainty for our analysis.

Note that both flare material and corona material can be accelerated in the same gradual event (e.g. Mason et al. 1999; Li & Zank 2005b; Li & Mewaldt 2009; Li et al. 2012; Mewaldt et al. 2012). In many large gradual SEP events, a notable feature is the initial strong enhancement of Fe/O ratios, sometimes reaching values of 1, comparable to impulsive SEP events. Such a strong enhancement at the beginning phase of a large SEP event has led many researchers (e.g. Reames et al. 1990; Cliver 1996; Cane et al. 2003; Li & Zank 2005b) to the examination of the so-called “hybrid” events, where particles accelerated at both flares and CME-driven shocks can contribute to the same SEP event. Later, Mason et al. (2006) noted that when the Fe time-intensity profiles were compared to those of O at a higher energy, the time profiles of Fe and O became very similar and yield Fe/O ratios that do not vary substantially with time. Mason et al. (2006) concluded that the initial peak of Fe/O ratio may be due to transport effect. In a follow up study, Mason et al. (2012) examined the effect of transport on the temporal evolution of SEP intensities for different heavy ions for 17 large SEP events. By employing a numerical transport model which includes the effects of pitch angle scattering, convection, adiabatic cooling, and magnetic focusing, the authors modeled the time intensity profiles of H, He, O and Fe at several energies from 386 keV/nuc to 40 MeV/nuc. The model calculation showed that the Fe/O ratio taking at different energies for Fe and O show little time variation, confirming the earlier results of Mason et al. (2006). Furthermore, the scaling of the energy is decided by the interplanetary turbulence. In another work, using observations of *Wind* and *Ulysses*, Tylka et al. (2013) also demonstrated that the initial enhancements of Fe/O are better understood as a transport effect, driven by the different mass-to-charge ratios of Fe and O.

While the instantaneous Fe/O ratio can vary largely as a function of time in an SEP event due to the fact that the transport process is  $Q/A$  dependent, the event-integrated Fe/O ratio does not depend on the transport process and therefore may still provide clues about the source of the seed population. If both flare material and coronal material can serve as the seed population for gradual SEP events, is there some dependence of the event intensity on the seed material? Do larger events tend to have more flare material or coronal material? In this paper, we address such questions using observations of major large gradual SEP events in solar cycle 23. Since many large SEP events are twin-CME events, our study are performed in the context of the twin-CME scenario.

Our paper is organized as follows: in section 2 we discuss the data selection and analysis procedure; in section 3 we present our analysis results; and section 4 contains the conclusion and discussion.

## 2. Data Selection

For large SEP events, we use the large proton event list from the NOAA “Solar Proton Events Affecting the Earth Environment” list (found at <http://www.swpc.noaa.gov/ftpdir/indices/SPE>) in the years 1997 through 2006. Note that in this list, a large proton event is defined with intensity  $> 10$  pfu (1 pfu= $1\text{proton cm}^{-2}\text{s}^{-1}\text{sr}^{-1}$ ) in the  $> 10$  MeV channel of the Geostationary Operational Environmental Satellites (GOES) instrument. In order to identify the source active region of solar energetic particles clearly, we only consider the events where the associated CMEs occur in the front-side hemisphere of the sun. SEP lists and GLE lists from Ding et al. (2013, 2014) and Li et al. (2012) are also used as the major event lists in this study. Since we are interested in the twin-CME scenario, the information about twin-CMEs of each SEP event in Ding et al. (2013) and Ding et al. (2014) are also used. For the twin-CME events, we follow the same identification criteria as Ding et al. (2014). The selected events and their properties are summarized in Table 1.

The first column in Table 1 shows the event number. The second and the third column are the date and the onset time of the SEP event. Column 4 and 5 are the onset time of the associated CME and its projection speed on the sky plane (from catalog at [http://cdaw.gsfc.nasa.gov/CME\\_list/](http://cdaw.gsfc.nasa.gov/CME_list/)). Column 6 is the NOAA active region (AR) number, and “?” denotes event that has no NOAA AR number. Column 7 is the location of the source active region at the onset time of CME eruption. The associated flare classes and onset times are shown in column 8 and 9, respectively, where ‘-’ denotes that no flares are identified. Column 10 is the peak proton flux intensity in the  $> 10\text{MeV}$  channel of GOES satellite of the SEP event.

Following Cane et al. (2006), we use 25-80MeV/nuc heavy ions (Fe and O) detected by the ACE/SIS (Stone et al. 1998) instrument in our study. As shown in Zank et al. (2000); Li et al. (2003), the maximum particle energy at a CME-driven shock quickly drops as the shock propagates out. For a particle with energy of 25-80MeV/nuc, it is likely accelerated near the Sun. So the Fe/O ratio in the energy range of 25-80MeV/nuc can largely reflect the near-sun seed population of the event. The Fe/O ratio was calculated by integrating the time-averaged SEP spectra from 25 to 80 MeV/nuc over the duration of the event. The time intervals used for obtaining the Fe/O ratio for each SEP event are given in column 11 and 12 in Table 1. Column 13 shows the event-integrated Fe/O ratio (normalized to the value 0.134) in the energy range 25-80 MeV/nuc. Column 14 and 15 are the solar energetic particle propagation path length ( $L$ ) from near the sun to 1 AU and the solar particle release height (SPR-H), respectively. The path length and the SPR-H are inferred from the ACE/SIS data by using the method of Velocity Dispersion Analysis (VDA) (e.g. (Tylka et al. 2003; Reames 2009a)). A symbol of ‘-’ denotes that there was not enough valid ACE/SIS data available

or that the results are unreasonable. For events where the SPR results are listed in Reames (2009a), we obtained similar results and have used the results as listed in Reames (2009a). Symbol ‘np’ in the column 16 indicates that no preceding CMEs within 13 hrs ahead of the main CME was found. These are “single-CME” events. Symbol ‘\*’ in the column 17 denotes GLE events.

### 3. Analyses and Results

For our analysis, we follow Ding et al. (2013) and categorize all SEP events to two groups: “single-CME” SEP events and “twin-CME” SEP events. Note that the preceding CMEs are often slower and narrower. If they are too slow, they may not drive a shock and consequently no particle acceleration can take place and there is no enhanced seed population nor enhanced turbulence level at the shock driven by the main CME. Therefore, in identifying the preceding CME, we require the speed of the CME to be larger than 300 km/sec so that the likelihood it drives a shock is larger. However, it has to be pointed out that there is no guarantee of a shock at the preceding CME. Consequently, as noted by Ding et al. (2013), some of the twin-CMEs we identified should be counted as single CMEs..

In the case that the preceding CME does drive a shock and there is particle acceleration and so enhanced seed population nor enhanced turbulence level, one may wonder which one, the seed population or the enhanced turbulence, is the more important factor in leading to a large SEP event. Such a question is hard to answer as neither the seed population nor the turbulence strength near the Sun is presently available. Perhaps in the very extreme events, both factors play a role. Incidentally, we note that enhanced seed particles from preceding CMEs may also exist in impulsive SEP events (see e. g. lists in (Reames et al. 2014; Reames 2014; Reames et al. 2015)).

#### 3.1. Longitudinal dependance of Fe/O

For these two types of SEP events, we first examine the longitudinal distribution of the event-integrated Fe/O (normalized to 0.134) in the energy range of 25-80MeV/nuc. This is shown in Figure 1. In panel (a) of Figure 1, the blue cycles denote “twin-CME” events, and the red triangles denote “single-CME” events. From the figure we can see that, for both “single-CME” and “twin-CME” events, the Fe/O ratio for events with western source regions are larger than those with eastern source region. If we acknowledge that a normalized event-integrated Fe/O  $> 2.0$  to be an indication of the presence of flare materials as the seed

population (Cane et al. 2006), then all, but two, events having flare material as seeds are from western hemisphere. This is consistent with the case study of Reames (2014), who noted that Fe-rich events tend to have shocks with western source. Also shown in panel (a) are the blue and red stair curves which are the mean Fe/O values in each bin of 30 degrees for the twin-CME events and the single-CME events, respectively. Clearly we can see that events with high mean Fe/O values occur mainly in the longitude range from 30 to 90 degrees. This is an interesting result. It suggests that the seed flare material may be very localized. We tend to see enhanced Fe/O ratio for western events because the magnetic connection to 1 AU is better for western events. For eastern events, because the seed flare material are not well-connected to Earth, so we do not see enhanced Fe/O ratio. This implies that if we observe large SEP events with multiple spacecraft that are separated in longitude (e.g. STEREO spacecraft), we may observe different event-integrated Fe/O ratio. Of course we do not know if the seed flare material is from the flare that accompanies the CME or from preceding flares.

It is also interesting to note that, except two well-connected single-CME events, the rest  $\text{Fe/O} > 2.0$  events are all twin-CME events. This is consistent with the twin-CME scenario in which the shock driven by the main CME not only can accelerate coronal/solar wind material that are pre-accelerated at the shock with the preceding CME, but also can accelerate flare material that are from flares associated with the preceding CMEs. Preceding flares may provide seed particles for the subsequent acceleration at the main CME-driven shock has been noted in the twin-CME scenario (Li et al. 2012; Ding et al. 2013).

We also note that for each longitude bin, the mean Fe/O ratio of twin-CME events is larger than that of single-CME events. This may be related to an important question concerning large SEP events: can particles accelerated at a flare be reaccelerated at the accompanying CME’s driven shock? If so, then the accompanying flare can provide seed particles for the CME-driven shock. Such a scenario has been examined in the simulation of (Li & Zank 2005b) where flare-accelerated particles are considered to be reaccelerated at the CME-driven shock. However, our result that most  $\text{Fe/O} > 2.0$  events are twin-CME events seems to suggest that particles accelerated at a flare may have a hard time to be re-accelerated by the accompanying CME-driven shock. Because if there is reacceleration, then single-CME event could have similar Fe/O ratio as twin-CME events. On the other hand, if flares only provide seed particles for subsequent CME-driven shocks but not the accompanying CME-driven shock, then we expect twin-CME events to have larger Fe/O ratio than single-CME events.

Panel (b) of Figure 1 shows the histogram of the normalized event-integrated Fe/O ratio, where the blue bars are for the twin-CME events, and the red ones are for the single-CME

events. While most single-CME events have the normalized Fe/O ratios below 2.0, a lot of twin-CME events have normalized Fe/O ratios between 2.0 and 4.0. This again suggests that the seed particles in single-CME events are mostly from solar wind/coronal materials while those in twin-CME events may have two sources: flare material from preceding flares and coronal/solar wind material from preceding CMEs.

### 3.2. SEP peak intensity and the normalized Fe/O ratio

The peak flux intensities of large SEP events are shown in Figure 2 as a function of the normalized event-integrated Fe/O ratios. Blue symbols denote twin-CME events and red symbols denote single-CME events. The result is very interesting. Consider first single-CME events. These events are clustered in the lower left part of the plot. Except for one event, all other 8 events have peak intensities smaller than 100 pfu. In the twin-CME scenario for large SEP events, the peak intensity is directly related to the seed population. Lacking a preceding CME, the seed population for single-CME event is presumably limited and therefore we do not expect to find large SEP peak intensity for these events. In comparison, twin-CME events show a much broader scatter of peak intensity: 14 events have peak intensities above 1000 pfu; 22 have peak intensities between 100 and 1000 pfu, and 21 have peak intensities between 10 and 100 pfu. Such a scattering is a natural conclusion of the twin-CME scenario in which the preceding CMEs, depending on its propagation direction, strength, how much time prior to the main CME, etc, can lead to a broad range of enhanced seed population and enhanced turbulence level at the subsequent shock driven by the main CME. Unfortunately, no in-situ observations of either the seed population or the turbulence strength near the Sun is presently available. We do not know which one, the seed population or the enhanced turbulence, is more important in leading to a large SEP event. Perhaps in the very extreme events, both factors play a role.

One fact to note is that for extremely large SEP events, defined here as events with peak intensities  $> 1000$ pfu, all but 1 (i.e. 13 out of 14) have normalized event-integrated Fe/O values  $< 2.0$ , indicating that the seed particles in these events are dominated by coronal material/solar wind. As we discussed in the last section, flare material from preceding flares can serve as seed particles at the shock driven by the main CME. So why extreme SEP events, which are all twin-CME events, and having preceding flares, have Fe/O ratios smaller than 2.0? This can be understood if shocks driven by pre-CMEs can provide more seed particles than pre-flares. This is possible because for flare seed particles (that are accelerated at the pre-flares) to be later accelerated at the shock driven by the main CME, these flare particles need to leak out to the interplanetary medium from the flare site first, through



perhaps interchange reconnection. In comparisons, coronal and solar wind material that are accelerated at the preceding shock can be processed by the main shock easily if both shocks are propagating towards similar directions. Consequently, pre-CMEs may provide more seed particles than pre-flares. Now an extremely large SEP event needs to have a large seed population, and since pre-CMEs can provide more seed population than pre-flares, we conclude that extreme events are those events where seed particles are efficiently and dominantly produced at pre-CMEs. Consequently the Fe/O ratios in extreme events are closer to coronal values than flare values. Along this reasoning, we would expect that in less extreme twin-CME events (e.g., events having peak intensities smaller than 1000 pfu), the Fe/O ratio will scatter and have a larger range. This is indeed what is shown in Figure 2. Finally note that all single-CME events (except one) have small Fe/O ratios since there is no contribution of flare seed material from pre-flares. A thumb rule of large SEP events from Figure 2 is therefore the following: a) single CMEs can rarely produce large SEP events with a peak intensity larger than 100 pfu and the Fe/O ratios in these events are often smaller than 2.0; b) large events having peak intensity larger than 100 pfu are almost all produced by twin-CMEs and the Fe/O ratio of these events have a large scattering range, can reach 8.0 if sufficient flare seed material presents; 3) for very large events having a peak intensity larger than 1000 pfu, the seed population is likely from pre-CMEs than pre-flares and therefore the Fe/O ratio becomes smaller again.

In the work of Ding et al. (2013), it was suggested that if the twin-CME scenario is the cause for large SEP events, then the peak flux intensity of these large SEP events (that are caused by twin-CMEs), which is mostly controlled by the seed population and the turbulence level at the shock driven by the main CME, should have little correlation with the associated flare class, or with the speed of the associated CMEs. For extreme SEP events, the correlation should be even less. Figure 3 plots the event peak intensity as functions of flare class and CME speed. The upper two panels are for all events and the lower two panels are for extreme events ( $I_p > 1000\text{pfu}$ ) only. The blue dashed lines in each panel are the linear fit to the result and the correlation coefficients are shown in each panel. Clearly, we can see from panel (c) and (d), for extreme SEP events there is no correlation between the peak intensity and the flare class or the CME speed. Even for all events (panel (a) and (b)), the dependence of peak intensity on either the flare class or the CME speed is at most tangential. Figure 3, therefore, provides further supports to the twin-CME scenario.

Consider now GLE events. In Figure 2, we also separate all twin-CME events to GLE events and non-GLE events. The blue squares denote the GLE events, and the blue circles denote non-GLE events. The red triangles denote single-CME events. Not surprisingly, the GLE events are often the more intense events for a given Fe/O ratio.

### 3.3. Solar Particle Release height

We now examine the solar particle release (SPR) height for our events. Using the VDA method (Tylka et al. 2003; Reames 2009a) and data from ACE/SIS, we derive the Solar Particle Release (SPR) time near the Sun. We then obtain the height of the associated CME from the speed of the CME (as given from the CDAW CME catalog [http://cdaw.gsfc.nasa.gov/CME\\_list/](http://cdaw.gsfc.nasa.gov/CME_list/)). To be clear, it is the height of the nose of the CME and we use it as a proxy of the height of the leading edge of the CME-driven shock. Note that only under the assumption that energetic particles are release near the nose of the CME driven shock, this height is the solar particle release (SPR) height. If energetic particles are released at the flank of the CME-driven shock, then this height is only the upper limit of the SPR height. In the following we refer this height as the SPR height. This height is shown as a function of the Fe/O ratio in Figure 4. As shown in the figure, it seems that events with higher Fe/O values have lower SPR heights. This can be understood as the following. First we note that the seed particles from pre-CMEs can exist in a larger region (reaching to a larger height) than pre-flares since the pre-CME is more extended that the pre-flare. Now since the SEPs are continuously accelerated at the shock driven by the main CME and since the seed particles from pre-CMEs occupy a larger region than pre-flares, so the larger the SPR height, the more pre-CME accelerated material (than pre-flare accelerated material) will be processed by the shock, thus a smaller Fe/O ratio. It is interesting to note that for GLE events, the SPR heights are low, 10 of them are below  $5R_s$  and 3 are between  $5R_s$  and  $10R_s$ . This agrees with earlier work of Reames (2009b), who first suggested that GLE events have lower SPR release height than non-GLE events. This result indicates that to generate a GLE event, where particles can be accelerated to  $\sim$  GeV/nuc in energy, there must be plenty of seed particles, either flare material or corona material, due to preceding flares and/or CMEs, to exist very low in the corona. This is not surprising since coronal shock strength quickly decreases with height and the maximum particle energy also decreases quickly with CME height (Zank et al. 2000; Li et al. 2003). So to get to  $\sim$  GeV/nuc in energy, the acceleration has to occur very low in corona.

## 4. Conclusions and Discussions

In this work, we examine the source of seed population in large gradual SEP events using event-integrated Fe/O ratios (normalized to the Reames value of 0.134) in the energy range of 25-80 MeV/nuc. The data is from the SIS instrument onboard ACE spacecraft are used. We assume that the element abundances of Fe and O in this energy range is consistent with those in the seed population. Following Cane et al. (2006) we use the normalized Fe/O

ratio  $> 2.0$  as the indicator of the presence of the flare materials.

We find that the SEP events with high Fe/O ( $> 2.0$ ) ratios almost always have western hemispheric source regions. Furthermore all events with Fe/O  $> 2.0$  are twin-CME events except one, and all single-CME events, except one, have the normalized Fe/O ratio  $\leq 2.0$ . For twin-CME events, the normalized Fe/O ratio have a larger scattering, and many events have Fe/O ratios  $> 2.0$ , indicating the presence of flare seed material that are likely from pre-flares. For any given longitude, the average Fe/O ratios in twin-CME events are higher than those in single-CME events.

These results are consistent with the two-CME scenario. In the twin-CME scenario, the turbulence excited by preceding CME shocks can keep seed particles accelerated at either preceding flares and preceding CME shocks near the Sun for a certain period, after which the seed particles can then undergo a second acceleration process at the main CME shock. Consequently, because the possibility of the presence of flare seed particles, we expect to see enhancement of Fe/O in some of these twin-CME events. In comparison, we expect to see no F/O enhancement in single-CME events.

It is interesting to find that for the most extremely large SEP events, defined as having  $I_p > 1000$  pfu, they are all twin-CME events, but they all have Fe/O  $\leq 2.0$  except one. We suggest that the reason for these events to have Fe/O  $\leq 2.0$  is because to generate these events the intensity of the seed particles has to be large and comparing to pre-flares, pre-CMEs can produce more seed particles, so the Fe/O ratio in these event are coronal like than flare like. Furthermore the event-integrated intensity for extreme events show no correlation with the flare class or the CME speed (as shown in Figure 3). This is predicted by the twin-CME scenario since in the twin-CME scenario the key factor to lead to a large SEP event is the seed population and/or the presence of strong turbulence, but not the flare class nor the CME speed.

Not surprisingly the intensity of GLE events is usually larger than those of SEP events, suggesting the seed population for GLE events is larger than non-GLE SEP events. We also examine the solar particle release height for twin-CME events (GLE and non-GLE events) and single-CME events. We find that events with higher Fe/O values tend to have lower SPR heights, confirming earlier results of Reames (2009b) for GLE events. This also agrees with the twin-CME scenario (see discussion in the last section). Furthermore, the SPR height for GLE events are often lower than  $5R_s$ , suggesting that to have a GLE event, plenty of seed particles must exist very low in the corona.

We are grateful to ACE/SIS, and CDAW CME catalogs for making their data available online. This work is supported at UAH by NSF grant AGS-1135432; at NUIST by NSFC-

41304150 for Ding L.G.; at CMA by NSFC-41074132, NSFC-41274193 for Le G.M.; and at NUIST by Jiangsu Government Scholarship for Overseas Studies (Grant No. JS2012-105) for Gu B..

## REFERENCES

- Cane, H., von Rosenvinge, T., Cohen, C., & Mewaldt, R. 2003, *Geophys. Res. Lett.*, 30, 5
- Cane, H. V., McGuire, R. E., & von Rosenvinge, T. T. 1986, *Astrophys. J.*, 301, 448
- Cane, H. V., Mewaldt, R. A., Cohen, C. M. S., & von Rosenvinge, T. T. 2006, *Journal of Geophysical Research*, 111, doi:1029/2005JA011071
- Cliiver, E. W. 1996, *AIP Conference Proceedings*, 374, 45
- Cliiver, E. W., Kahler, S. W., & Reames, D. V. 2004, *The Astrophysical Journal*, 605, 902
- Ding, L., Jiang, Y., Zhao, L., & Li, G. 2013, *The Astrophysical Journal*, 763, 30
- Ding, L.-G., Li, G., Dong, L.-H., et al. 2014, *Journal of Geophysical Research: Space Physics*, 119, 1463
- Giacalone, J. 2005a, *The Astrophysical Journal*, 624, 765
- Giacalone, J. 2005b, *The Astrophysical Journal Letters*, 628, L37
- Giacalone, J. & Ellison, D. 2000, *Journal of Geophysical Research: Space Physics*, 105, 12541
- Gopalswamy, N., Yashiro, S., & Krucker, S. 2004, *Journal of Geophysical Research*, 109, 1
- Gopalswamy, N., Yashiro, S., Michäk, G., et al. 2002, *The Astrophysical Journal Letters*, 572, L103
- Kahler, S. W., Sheeley, N. R., Howard, R. A., et al. 1984, *Journal of Geophysical Research: Space Physics*, 89, 9683
- Kahler, S. W. 1996, *AIP Conference Proceedings*, 374, 61
- Kahler, S. W., Reames, D. V., & Burkepille, J. T. 2000, *ASP Conference*, 206, 468
- Kahler, S. W., & Vourlidas, A. 2013, *The Astrophysical Journal*, 769, 143
- Li, G., & Mewaldt, R. A. 2009, *Proceedings of the 31st ICRC, SH*, paper no: 1362

- Li, G., Moore, R., Mewaldt, R. A., Zhao, L., & Labrador, A. W. 2012, *Space Science Reviews*, 171, 141
- Li, G., & Zank, G. P. 2005a, 29th ICRC proceedings, 1, 173
- Li, G., & Zank, G. P. 2005b, AIP Conference Proceedings, 233
- Li, G., Zank, G. P., & Rice, W. K. M. 2003, *J. Geophys. Res.*, 108, 1082
- Mason, G. M., Desai, M. I., Cohen, C. M. S., et al. 2006, *The Astrophysical Journal Letters*, 647, L65
- Mason, G. M., Dwyer, J. R., & Mazur, J. E. 2000, *Astrophysical Journal*, 545, L157
- Mason, G. M., Li, G., Cohen, C. M. S., et al. 2012, *The Astrophysical Journal*, 761, 104
- Mason, G. M., Mazur, J. E., & Dwyer, J. R. 1999, *Astrophys. J. Lett.*, 525, L133
- Mewaldt, R., Looper, M., Cohen, C., et al. 2012, *Space Science Reviews*, 171, 97
- Reames, D. V. 1995, *Reviews of Geophysics*, 33, 585
- Reames, D. V. 1998, in *Space Sciences Series of ISSI, Vol. 5, Solar Composition and its Evolution - from Core to Corona*, ed. C. Fröhlich, M. Huber, S. Solanki, & R. Steiger (Springer Netherlands), 327–340
- Reames, D. V. 1999, *Space Science Review*, 90, 413
- Reames, D. V. 2009a, *The Astrophysical Journal*, 693, 812
- Reames, D. V. 2009b, *The Astrophysical Journal*, 706, 844
- Reames, D. V. 2014, *Solar Physics*, 289, 977, DOI: 10.1007/s11207-013-0350-4
- Reames, D. V., Cliver, E. W., & Kahler, S. W., 2015, *Solar Physics*, 290, 1761
- Reames, D. V., Cliver, E. W., & Kahler, S. W. 2014, *Solar Physics*, 289, 3817
- Reames, D. V., Cane, H. V., & Von Roseninge, T. 1990, *Astrophysical Journal*, 357, 259
- Reames, D. V., & Ng, C. K. 2004, *Astrophys. J.*, 610, 510
- Stone, E., Frandsen, A., Mewaldt, R., et al. 1998, in *The Advanced Composition Explorer Mission* (Springer), 1–22
- Tylka, A. J., Cohen, C. M. S., Dietrich, W. F., et al. 2005, *Astrophysical Journal*, 625, 474

Tylka, A., Malandraki, O., Dorrian, G., et al. 2013, *Solar Physics*, 285, 251

Tylka, A. J., & Lee, M. A. 2006, *Astrophysical Journal*, 646, 1319

Tylka, A. J., Cohen, C. M. S., Dietrich, W. F., et al. 2003, *28th ICRC Proceedings*, 6, 3305

Zank, G. P., Rice, W. K. M., & Wu, C. C. 2000, *Journal of Geophysical Research-Space Physics*, 105, 25079

Table 1: The properties of the large SEP events (solar cycle 23)

No.	SEP		CME onset	$V_{CME}$ (km/s)	AR (NOAA)	loc.	flare		Ip (pfu)	summing interval <sup>a</sup>		Fe/O <sup>b</sup> (SIS)	$L^c$ (AU)	SPR-H <sup>d</sup> ( $R_s$ )	comm. <sup>e</sup>
	date	time					FC	onset		start	end				
(1)	(2)	(3)	(4)	(5)	(6)	(7)	(8)	(9)	(10)	(11)	(12)	(13)	(14)	(15)	(16)
1	1997/11/04	07:00	06:10	785	8100	S14W33	X2.1	05:52	72	11/04 06:00	11/06 09:00	3.12	2.85	1.44	np
2	1997/11/06	13:00	12:11	1556	8100	S18W63	X9.4	11:49	490	11/06 12:00	11/09 20:00	6.47	2.55	8.56	*
3	1998/05/02	14:00	14:06	938	8210	S15W15	X1.1	13:31	150	05/02 14:00	05/04 18:00	4.96	1.24	2.90	*
4	1998/05/06	08:25	08:29	1099	8210	S11W65	X2.7	07:58	210	05/06 08:00	05/08 05:00	3.66	1.10	1.76	*
5	1999/06/04	08:00	07:27	2230	8552	N17W69	M3.9	06:52	64	06/04 07:00	06/06 04:00	2.89	2.04	3.36	
6	2000/04/04	17:00	16:33	1188	8933	N16W66	C9.7	15:12	55	04/04 16:00	04/07 00:00	0.90	1.66	11.04	
7	2000/06/10	18:00	17:08	1108	9026	N22W38	M5.2	16:40	46	06/10 17:00	06/12 03:00	5.94	1.23	2.97	
8	2000/07/14	11:00	10:54	1674	9077	N22W07	X5.7	10:03	24000	07/14 11:00	07/18 19:00	0.89	1.71	2.60	*
9	2000/07/22	12:00	11:54	1230	9085	N14W56	M3.7	11:17	17	07/22 12:00	07/23 08:00	0.41	1.78	2.48	np
10	2000/09/12	13:00	11:54	1550	9163	S17W09	M1.0	11:30	320	09/12 13:00	09/15 23:00	3.84	1.61	12.93	
11	2000/10/25	12:00	08:26	770	9199	N10W66	C4.0	08:45	15	10/25 13:00	10/27 21:00	0.68	1.57	9.88	
12	2000/11/08	23:30	23:06	1738	9213	N10W77	M7.4	22:42	14800	11/08 23:00	11/13 00:00	0.05	1.20	7.18	
13	2000/11/24	16:00	15:30	1245	9236	N22W07	X2.3	14:51	940	11/24 16:00	11/25 22:00	2.46	1.07	8.03	
14	2001/01/28	17:00	15:54	916	9313	S04W59	M1.5	15:40	49	01/28 17:00	01/31 00:00	5.07	-	-	
15	2001/03/29	11:00	10:26	942	9393	N20W19	X1.7	09:57	35	03/29 11:00	04/01 00:00	3.42	-	-	
16	2001/04/02	23:00	22:06	2505	9393	N18W82	X2.0	21:32	1100	04/02 23:00	04/07 12:00	2.68	1.11	10.63	
17	2001/04/10	08:00	05:30	2411	9415	S23W09	X2.3	05:06	355	04/10 08:00	04/12 12:00	1.18	2.52	8.28	
18	2001/04/12	12:00	10:31	1184	9415	S19W42	X2.0	09:39	51	04/12 12:00	04/14 00:00	2.01	2.11	6.96	np
19	2001/04/15	14:00	14:07	1199	9415	S20W85	X1.4	13:19	951	04/15 14:00	04/18 00:00	6.04	1.70	2.4	*
20	2001/09/15	12:00	11:54	478	9608	S21W49	M1.5	11:04	11	09/15 12:00	09/16 06:00	0.78	2.30	2.28	np
21	2001/10/01	13:00	05:30	1405	9628	S20W84	M9.1	04:41	2360	10/01 13:00	10/03 06:00	0.83	-	-	
22	2001/10/19	17:30	16:50	901	9661	N15W29	X1.6	16:13	11	10/19 18:00	10/21 20:00	1.77	-	-	
23	2001/11/04	17:00	16:35	1810	9684	N06W18	X1.0	16:03	31700	11/04 17:00	11/09 13:00	0.44	1.95	8.06	*
24	2001/11/23	00:00	23:30	1437	9704	S15W34	M9.9	22:32	18900	11/23 00:00	11/26 23:00	0.71	-	-	
25	2001/12/26	05:30	05:30	1446	9742	N08W54	M7.1	04:32	779	12/26 06:00	12/28 22:00	5.46	1.64	3.6	*
26	2002/01/14	06:00	05:35	1492	?	S28W83	M4.4	05:29	15	01/14 06:00	01/17 00:00	0.72	1.70	2.46	np
27	2002/02/20	06:30	06:30	952	9825	N12W72	M5.1	05:52	13	02/20 06:00	02/21 12:00	6.42	1.47	1.91	
28	2002/03/16	03:00	23:06	957	9866	S08W03	M2.2	22:09	13	03/16 03:00	03/17 16:00	0.95	-	-	np
29	2002/03/18	06:00	02:54	989	9866	S09W46	M1.0	02:16	53	03/18 06:00	03/20 09:00	1.10	-	-	
30	2002/04/17	10:30	08:26	1240	9906	S14W34	M2.6	07:46	24	04/17 11:00	04/18 20:00	1.72	1.31	12.23	np
31	2002/04/21	02:00	01:27	2393	9906	S14W84	X1.5	00:43	2520	04/21 02:00	04/25 00:00	0.23	1.68	3.12	
32	2002/05/22	06:00	03:50	1557	9948	S15W70	C5.0	03:18	820	05/22 06:00	05/25 00:00	0.65	-	-	
33	2002/07/16	10:30	21:30	1300	10030	N19W01	M1.8	21:03	234	07/16 11:00	07/19 08:00	1.59	-	-	
34	2002/08/14	03:00	02:30	1309	10061	N09W54	M2.3	01:47	26	08/14 01:00	08/15 22:00	1.40	1.35	3.33	np
35	2002/08/22	02:30	02:06	998	10069	S07W62	M5.4	01:47	36	08/22 02:00	08/23 06:00	5.30	1.69	2.62	
36	2002/08/24	01:30	01:27	1913	10069	S02W81	X3.1	00:49	317	08/24 02:00	08/27 00:00	6.47	2.16	2.4	*

Table 1 (Continued)

No.	SEP		CME onset	$V_{CME}$ (km/s)	AR (NOAA)	loc.	flare		Ip (pfu)	summing interval <sup>a</sup>		Fe/O <sup>b</sup> (SIS)	$L^c$ (AU)	SPR-H <sup>d</sup> ( $R_s$ )	comm. <sup>e</sup>
	date	time					FC	onset		start	end				
(1)	(2)	(3)	(4)	(5)	(6)	(7)	(8)	(9)	(10)	(11)	(12)	(13)	(14)	(15)	(16)
37	2002/09/06	04:00	02:06	737	10095	N08W31	-	-	208	09/06 04:00	09/09 00:00	0.53	-	-	
38	2002/11/09	15:00	13:32	1838	10180	S12W29	M4.6	13:08	404	11/09 15:00	11/11 12:00	0.64	2.20	9.09	
39	2003/05/28	04:00	00:50	1366	10365	S07W20	X3.6	00:17	121	05/28 04:00	05/30 03:00	2.07	2.24	19.54	
40	2003/05/31	02:40	02:30	1835	10365	S07W65	M9.3	02:13	27	05/31 03:00	06/01 00:00	3.37	1.85	1.54	
41	2003/10/26	18:25	17:54	1537	10484	N04W43	X1.2	17:21	466	10/26 17:00	10/27 22:00	1.67	1.28	2.10	
42	2003/10/29	21:00	20:54	2029	10486	S15W02	X10	20:37	1570	10/29 21:00	11/01 12:00	1.21	1.75	5.7	*
43	2003/11/02	11:00	09:30	2036	10486	S17W55	-	-	30	11/02 10:00	11/02 17:00	1.25	1.42	16.55	
44	2003/11/02	18:00	17:30	2598	10486	S14W56	X8.3	17:03	1570	11/02 18:00	11/04 20:00	0.94	1.83	3.57	*
45	2003/11/04	22:25	19:54	2657	10486	S19W83	X17	19:29	353	11/04 23:00	11/07 06:00	0.68	2.41	18.27	
46	2003/11/20	08:30	08:06	669	10501	N01W08	M9.6	07:35	13	11/20 08:00	11/21 12:00	1.26	-	-	
47	2003/12/02	12:30	10:50	1393	10508	S19W89	C7.2	09:40	86	12/02 13:00	12/04 10:00	1.00	-	-	
48	2004/04/11	06:00	04:30	1645	10588	S16W46	C9.6	03:54	35	04/11 06:00	04/12 20:00	3.02	-	-	
49	2004/07/25	18:55	14:54	1333	10652	N08W33	M1.1	14:19	2086	07/25 18:00	07/28 13:00	0.39	-	-	
50	2004/11/07	18:00	16:54	1759	10696	N09W17	X2.0	15:42	495	11/07 18:00	11/09 16:00	0.61	1.89	9.75	
51	2004/11/10	03:00	02:26	3387	10696	N09W49	X2.5	01:59	300	11/10 03:00	11/15 00:00	1.51	1.61	8.85	
52	2005/01/16	00:10	23:07	2861	10720	N15W05	X2.6	22:25	365	01/16 00:00	01/17 09:00	0.36	1.91	14.10	
53	2005/01/17	13:05	09:54	2547	10720	N15W25	X3.8	09:42	5040	01/17 13:00	01/19 08:00	0.18	-	-	*
54	2005/01/20	07:00	06:54	882	10720	N14W61	X7.1	06:36	1680	01/20 07:00	01/22 00:00	1.75	1.19	2.6	*
55	2005/07/13	17:00	14:30	1423	10786	N08W79	M5.0	14:01	13	07/13 17:00	07/14 10:00	0.51	-	-	
56	2005/08/22	19:30	17:30	2378	10798	S12W60	M5.6	16:46	330	08/22 20:00	08/26 00:00	0.58	-	-	
57	2006/12/13	03:10	02:54	1774	10930	S06W23	X3.4	02:14	698	12/13 03:00	12/14 20:00	7.12	1.72	3.8	*
58	2006/12/14	22:55	22:30	1042	10930	S06W46	X1.5	21:07	215	12/14 23:00	12/16 18:00	5.38	1.77	2.14	
E1	2000/06/06	19:00	15:54	1119	9026	N20E18	X2.3	14:58	84	06/06 22:00	06/10 00:00	2.68	2.15	11.49	
E2	2001/08/09	19:00	21:30	909	9570	S17E19	C7.8	18:22	17	08/09 19:00	08/11 12:00	0.16	-	-	
E3	2001/09/24	11:00	10:31	2402	9632	S16E23	X2.6	09:32	12900	09/24 11:00	10/01 00:00	0.14	-	-	
E4	2001/10/22	17:00	15:06	1336	9672	S21E18	M6.7	14:27	24	10/22 17:00	10/26 01:00	4.64	2.58	7.00	
E5	2001/11/17	06:00	05:30	1379	9704	S13E42	M2.8	04:49	34	11/17 12:00	11/22 12:00	0.39	-	-	
E6	2003/06/18	10:00	23:18	1813	10386	S08E58	M6.8	22:27	24	06/18 10:00	06/20 18:00	0.34	-	-	
E7	2003/10/28	12:00	11:30	2459	10486	S16E08	X17	11:00	29500	10/28 11:00	10/29 20:00	0.13	1.38	4.3	*
E8	2005/09/13	23:30	20:00	1866	10808	S09E10	X1.5	19:19	120	09/13 23:00	09/16 22:00	0.47	-	-	np

<sup>a</sup> the time interval of calculating the event-integrated Fe/O;

<sup>b</sup> the normalized value of event-integrated Fe/O in the range of 25-80MeV (SIS) (normalized to Reames value 0.134);

<sup>c</sup> the path length of SEP propagating from the sun to the spacecraft deduced by the VDA method; '-' denote that there is no credible and reasonable results, or no enough valid ACE/SIS data;

<sup>d</sup> the solar particle release height of SEP deduced by VDA and CME speed, and '-' denote that there is no credible and reasonable results, or no enough valid ACE/SIS data;

<sup>e</sup> '\*' denote the GLE events, and 'np' denote the SEP events (called single-CME events) that have no identified preceding CMEs within 13 hrs ahead of the associated fast and wide CME.



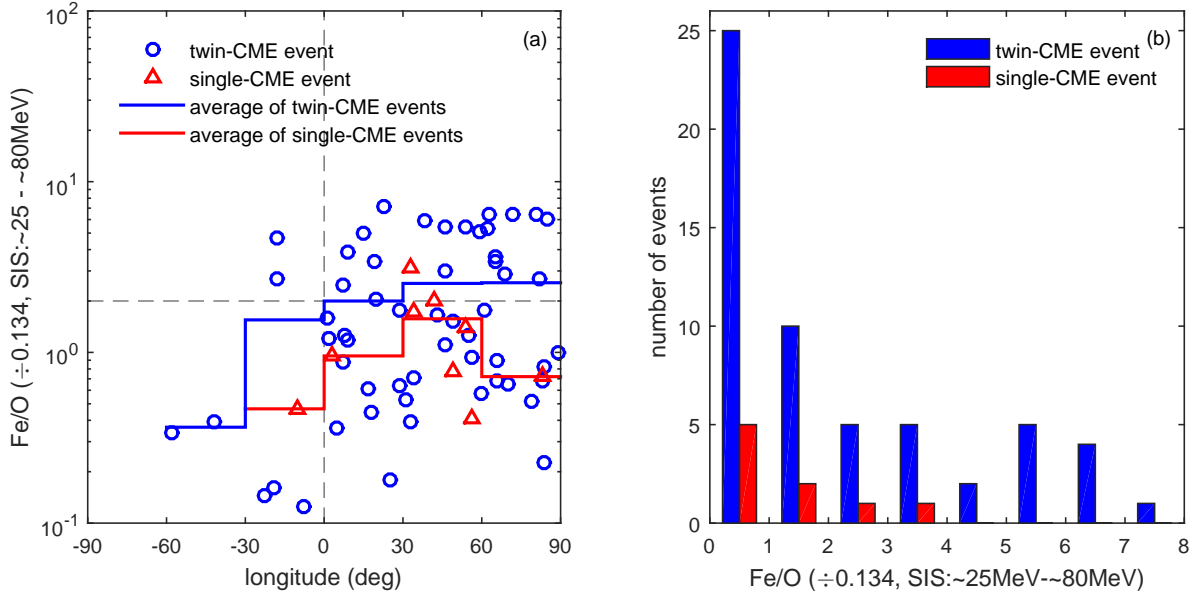


Fig. 1.— (a) Longitudinal distribution of the event-integrated Fe/O ratio in the energy range 25-80 MeV/nuc (normalized to Reames value, 0.134) of SEP events. The blue circles denote the events produced by the twin-CME eruptions, and red triangles denote the events produced by the single-CME eruptions. The stair curves indicate the mean Fe/O values for each group in each longitude bin, where the blue ones represent the twin-CME events and the red ones represent the single-CME events. (b) Histogram of the normalized Fe/O ratio of SEP events. The blue color show the twin-CME events, and the red color show the single-CME events.

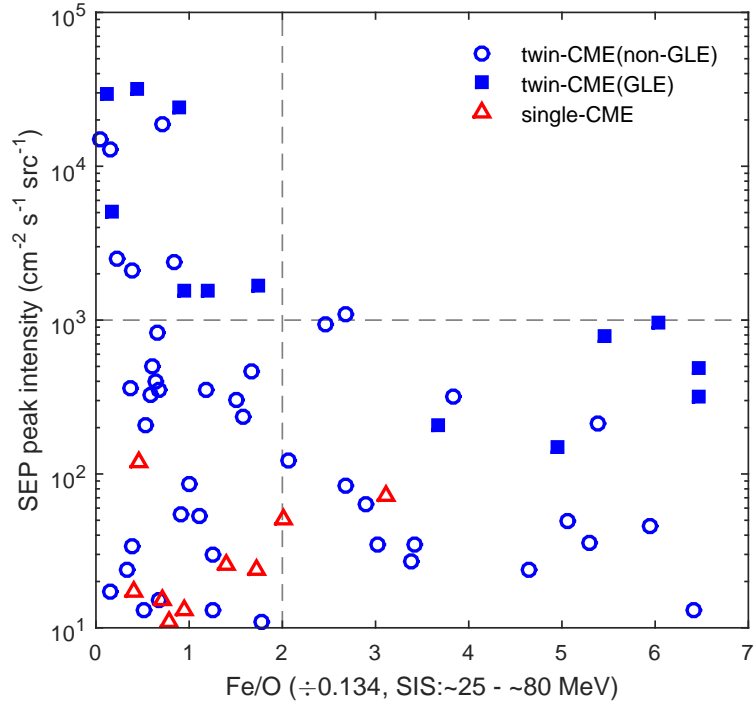


Fig. 2.— Peak intensity of large SEP event plotted versus normalized Fe/O ratio. Blue and red Symbols indicate the large SEP events associated with twin-CME events and single-CME events respectively. The blue circles denote the non-GLE SEP events, and the blue squares denote the GLE events.

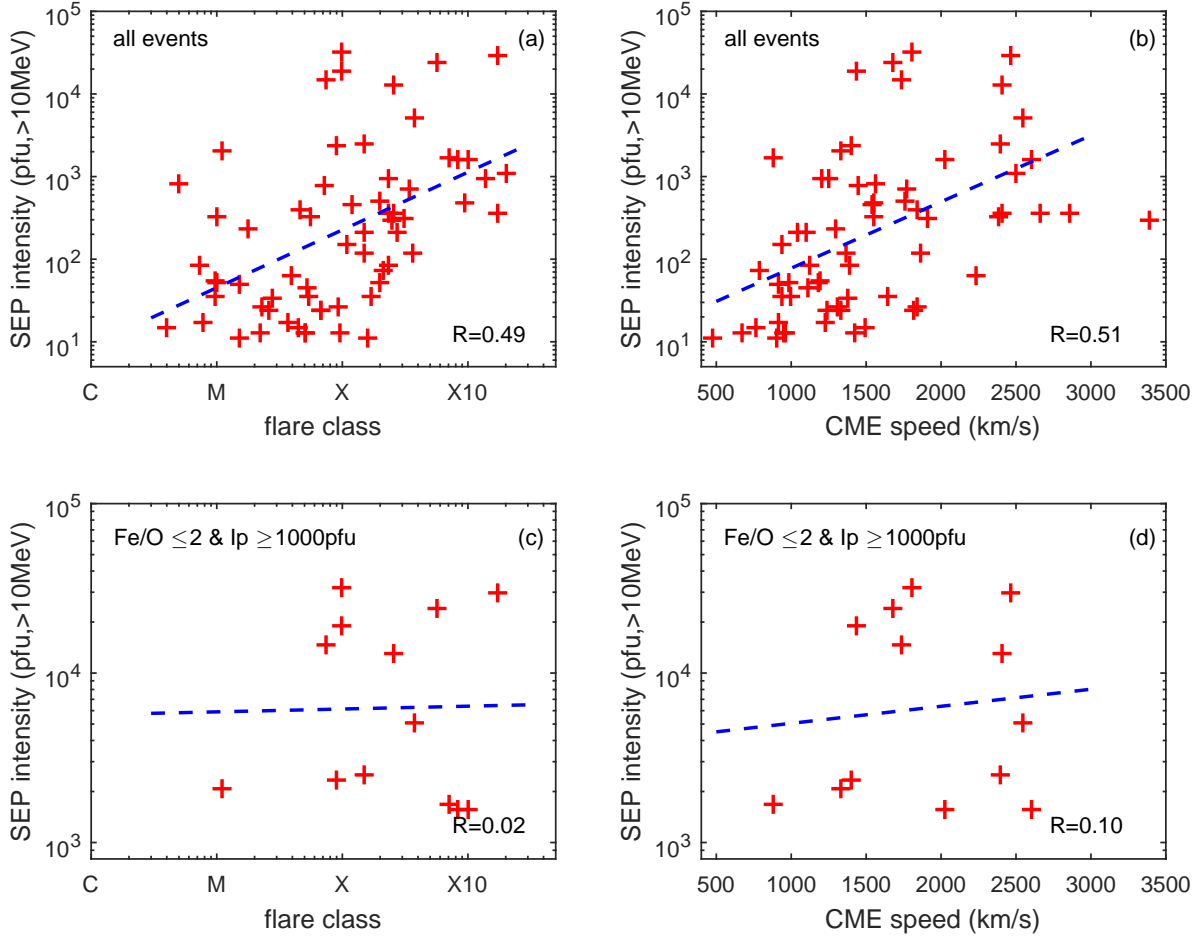


Fig. 3.— Peak intensity of large SEP event plotted versus the associated flare class and CME speed for all SEP events and extremely large SEP events. The blue line is the linear fit curve.

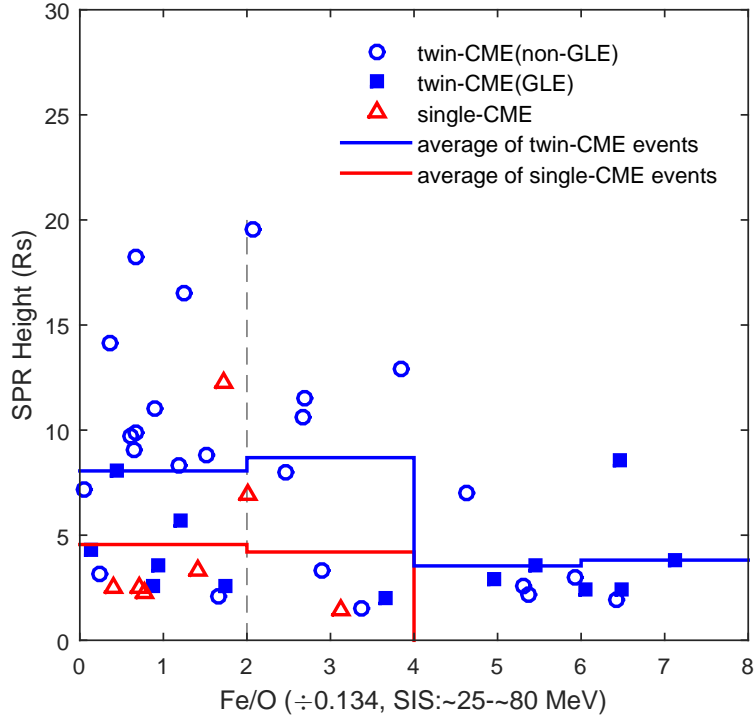


Fig. 4.— The solar particle release (SPR) height near the sun in each SEP event plotted versus the Fe/O ratio value. The blue and red symbols denote the twin-CME events and single-CME events respectively. The circles indicate the non-GLE SEPs, and the squares indicate the GLEs. The blue stairs show the mean SPR height in each Fe/O bin for twin-CME events, and the red stairs for single-CME events.